This article was downloaded by: [Chongqing University]
On: 14 February 2014, At: 13:28
Publisher: Taylor & Francis
Informa Ltd Registered in England and Wales Registered Number: 1072954 Registered office: Mortimer House, 37-41 Mortimer Street, London W1T 3JH, UK

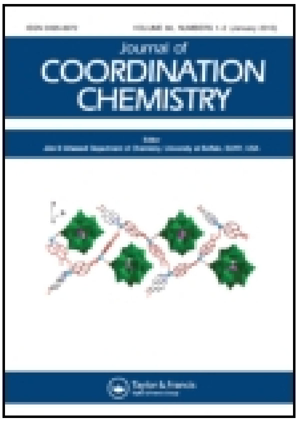

Journal of Coordination Chemistry
Publication details, including instructions for authors and subscription information:
http://www.tandfonline.com/loi/gcoo20

Synthesis, structure, and photoluminescence of a (4,6)-connected Cu(I)-CN-triazolate framework built with a unique heptanuclear hybrid cluster

Quan-Guo Zhai[a], Cheng-Feng Zhang[a], Shu-Ni Li[a], Yu-Cheng Jiang[a] & Man-Cheng Hu[a]

[a] Key Laboratory of Macromolecular Science of Shaanxi Province, School of Chemistry and Chemical Engineering, Shaanxi Normal University, Xi' an, P.R. China

Accepted author version posted online: 28 Oct 2013.Published online: 26 Nov 2013.

To cite this article: Quan-Guo Zhai, Cheng-Feng Zhang, Shu-Ni Li, Yu-Cheng Jiang & Man-Cheng Hu (2013) Synthesis, structure, and photoluminescence of a (4,6)-connected Cu(I)-CN-triazolate framework built with a unique heptanuclear hybrid cluster, Journal of Coordination Chemistry, 66:22, 4004-4014, DOI: 10.1080/00958972.2013.858810

To link to this article: http://dx.doi.org/10.1080/00958972.2013.858810

PLEASE SCROLL DOWN FOR ARTICLE

Taylor & Francis makes every effort to ensure the accuracy of all the information (the "Content") contained in the publications on our platform. However, Taylor & Francis, our agents, and our licensors make no representations or warranties whatsoever as to the accuracy, completeness, or suitability for any purpose of the Content. Any opinions and views expressed in this publication are the opinions and views of the authors, and are not the views of or endorsed by Taylor & Francis. The accuracy of the Content should not be relied upon and should be independently verified with primary sources of information. Taylor and Francis shall not be liable for any losses, actions, claims, proceedings, demands, costs, expenses, damages, and other liabilities whatsoever or howsoever caused arising directly or indirectly in connection with, in relation to or arising out of the use of the Content.

This article may be used for research, teaching, and private study purposes. Any substantial or systematic reproduction, redistribution, reselling, loan, sub-licensing, systematic supply, or distribution in any form to anyone is expressly forbidden. Terms &

Journal of Coordination Chemistry, 2013
Vol. 66, No. 22, 4004–4014, http://dx.doi.org/10.1080/00958972.2013.858810

Synthesis, structure, and photoluminescence of a (4,6)-connected Cu(I)–CN–triazolate framework built with a unique heptanuclear hybrid cluster

QUAN-GUO ZHAI*, CHENG-FENG ZHANG, SHU-NI LI, YU-CHENG JIANG and MAN-CHENG HU

Key Laboratory of Macromolecular Science of Shaanxi Province, School of Chemistry and Chemical Engineering, Shaanxi Normal University, Xi’ an, P.R. China

(*Received 17 May 2013; accepted 20 September 2013*)

A 3-D Cu(I)–CN–triazolate hybrid coordination polymer, $\{Cu_9(NH_2\text{-BPT})_2(BPT)_2(CN)_7\}_n$ (**1**) (NH_2-BPT = 4-amino-3,5-bis(3-pyridyl)-1,2,4-triazole, BPT = 3,5-bis(3-pyridyl)-1,2,4-triazole), has been synthesized via self-assembly of NH_2-BPT, CuCN, and $K_3Fe(CN)_6$ under hydrothermal conditions. Single-crystal X-ray diffraction data show that four of the five independent copper centers in **1** have a three-coordinated trigonal coordination geometry, and the remaining copper center has a two-coordinated linear geometry. Three Cu ions are linked by one *cisoid*-BPT and two CN^- to form a 16-membered ring subunit, which is joined by the two-coordinate copper center via the triazole N(4)-position to generate an unprecedented $[Cu_7(BPT)_2(CN)_4]$ hybrid heptanuclear cluster. Each heptanuclear motif is linked to two adjacent $[Cu_7]$ clusters through four CN^- anions, and further to four [Cu–CN–Cu] binuclear clusters through two *transoid*-NH_2-BPT ligands. Each of these [Cu–CN–Cu] units is linked to four neighboring heptanuclear motifs. The overall geometry is a 3-D (4,6)-connected topological framework with Schläfli symbol of $(4^4 \times 6^2)(4^4 \times 6^{10} \times 8)$. Compound **1** also exhibits high thermal stability and strong green fluorescence emission at 536 nm in the solid state.

Keywords: Copper cyanide; 4-amino-3,5-bis(3-pyridyl)-1,2,4-triazole; Heptanuclear cluster; Coordination polymer; Photoluminescence

1. Introduction

Organic–inorganic hybrid crystalline solids have attracted contemporary interest because they promise both diverse structural chemistry and multifunctional properties due to the combination of the characteristics of the organic and inorganic components [1–6]. It is well known that the properties of such hybrid solids are heavily influenced by their crystal structures. Undoubtedly, the investigation of the factors influencing the construction of hybrid solids is significant. Up to now, a large number of organic–inorganic hybrid frameworks with interesting structures and excellent properties have been reported; however, it still remains a challenging task to explore effective synthetic strategies for the preparation of crystalline hybrid materials with expected structure and properties [7]. The structures and properties of such organic–inorganic hybrids are mainly controlled by their

---

*Corresponding author. Email: zhaiqg@snnu.edu.cn

inorganic units and organic ligands. Among various inorganic components, copper cyanide systems have received special interest due to their fascinating structural frameworks, physical and chemical properties, and potential applications in many fields [8–11]. The $[Cu_a(CN)_b]$ cuprous cyanide skeletons generally exhibit rich structural motifs ranging from discrete oligomers to polymeric chains and 2-D layers. Copper cyanide clusters or polymers are facile secondary building units for constructing extended organic–inorganic hybrid architectures varying from one to three dimensions. In these cuprous cyanide hybrid structures, the organic components acting as linkers are usually multidentate nitrogen-donor ligands such as polypyridine and polyazaheteroaromatic compounds including pyrazole, imidazole, triazole, tetrazole, and benzotriazole [12–15]. Recently, the modification of 4,4′-dipyridine by introducing polyazaheteroaromatic spacers between the terminal pyridyl groups produced a new class of angular dipyridine derivatives, represented by 2,5-bis(2-,3-/4-pyridyl)-1,3,4-oxadiazole and 4-amino-3,5-bis(2-,3-/4-pyridyl)-1,2,4-triazole. These linkers can adopt versatile coordination modes and have produced many new types of coordination polymers with open channels, interesting luminescent properties, and unprecedented topologies [16–20]. Using the 4-amino-3,5-bis(3-pyridyl)-1,2,4-triazole (NH_2-BPT) ligand, we have reported a series of Ag(I) coordination polymers varying from a 2-D 6-connected 3^6 network to a 3-D cationic framework with *dia*-topology [21, 22]. Moreover, two 3-D hybrid supramolecular isomers with large $[Mo_8O_{26}]^{4-}$ clusters introduced by the configurations of the NH_2-BPT ligand have also been successfully isolated [23]. As an extension of our research work, NH_2-BPT was selected to construct new hybrid solids based on copper cyanide inorganic subunits. In this contribution, the self-assembly of CuCN, $K_3Fe(CN)_6$, and NH_2-BPT under hydrothermal conditions is shown to produce a 3-D coordination polymer $\{Cu_9(NH_2\text{-BPT})_2(BPT)_2(CN)_7\}_n$ (**1**), which exhibits a (4,6)-connected topology based on a unique $[Cu_7(BPT)_2(CN)_4]$ hybrid heptanuclear cluster and which was characterized by elemental analysis, FT-IR and Raman spectroscopy, powder X-ray diffraction (PXRD), single-crystal X-ray diffraction, TG/DTA, and photoluminescence measurements. To the best of our knowledge, although the hybrid copper halide system with NH_2-BPT or similar angular dipyridine derivatives has been extensively investigated, only one 2-D organic–inorganic hybrid network construction with NH_2-BPT has been reported to date [24].

2. Experimental setup

2.1. *Materials and physical measurements*

The NH_2-BPT ligand was prepared according to the literature method [25]. Other chemicals were of reagent grade and used without purification. C, H, and N elemental analyzes were determined on an Elementar Vario EL III elemental analyzer. PXRD data were collected on a Bruker D8 diffractometer. The simulated pattern was calculated from X-ray single-crystal diffraction data using the free Mercury 2.3 program provided by the Cambridge Crystallographic Data Center. Solid state fluorescence spectra were measured with a Cary Eclipse fluorescence spectrophotometer at room temperature. The Raman spectra were recorded using an ALMEGA Dispersive Raman spectrometer with the laser wavelength of 532 nm. The FT-IR spectra (KBr pellets) were recorded on a Nicolet Avatar 360 FT-IR spectrometer from 4000 to 400 cm^{-1}. Thermal stability studies were performed on a NETSCHZ STA−449C thermal analyzer from 40 to 1000 °C with a heating rate of 5 °C/min under nitrogen. The solid state photoluminescence was measured at room temperature using a Cary Eclipse fluorescence spectrophotometer with the excitation slit and emission slit both 2.5 nm.

2.2. *Synthesis of* $\{Cu_9(NH_2\text{-}BPT)_2(BPT)_2(CN)_7\}_n$ *(1)*

A mixture of CuCN (0.135 g, 1.5 mM), NH_2-BPT (0.12 g, 0.5 mM), $K_3Fe(CN)_6$ (0.165 g, 0.5 mM), and water was sealed in a Teflon-lined stainless steel vessel (15 mL), which was heated at 180 °C for 5 days under autogenous pressure and then cooled slowly (5 °C h^{-1}) to room temperature. Yellow block-shaped crystals were collected (0.15 g, 72% yield based on NH_2-BPT). Anal. Calcd (%) for $C_{55}H_{36}N_{29}Cu_9$: C, 39.44; H, 2.16; N, 24.25. Found (%): C, 39.51; H, 2.11; N, 24.33. FT-IR (cm^{-1}): 3344(m), 3162(w), 3062(w), 2923(w), 2851(w), 2125(s), 1598(w), 1580(s), 1473(w), 1454(m), 1438(w), 1409(s), 1325(m), 1199(m), 1163 (w), 1132(w), 1119(w), 1093(w), 1049(w), 1031(m), 1015(m), 961(m), 852(w), 814(m), 804(m), 756(m), 710(s), 693(s), 639(m), 607(w), 476(w), 421(w). Raman (cm^{-1}): 3071(w), 2130(s), 1601(s), 1508(m), 1451(w), 1421(w), 1019(s).

2.3. *Crystal structure determination*

Single-crystal X-ray diffraction data for **1** were collected with a Bruker Smart Apex-II CCD diffractometer with graphite-monochromated Mo $K\alpha$ radiation (λ = 0.71073 Å) at T = 293 (2) K. Empirical absorption corrections were applied using SADABS [26]. The structure was solved using direct methods and refined by full-matrix least-squares on F^2 by using the *SHELXL*-97 program package [27]. All nonhydrogen atoms were refined anistropically, and hydrogens were located and refined in their located positions. The μ_2-bridging cyanide groups between two Cu^I atoms indicated disorder with respect to the C and N termini; this disorder was treated by adopting 50% C and N occupancies at those sites. The disordered C/N positions are labeled as X. Crystal data as well as details of data collection and refinement for **1** are summarized in table 1. Selected bonded lengths and angles are listed in table 2.

Table 1. Crystal data, data collection, and structure refinement parameters for **1**.

Empirical formula	$C_{55}H_{36}N_{29}Cu_9$
Formula weight	1674.99
Crystal system	Triclinic
Space group	$P-1$
a (Å)	7.5001(15)
b (Å)	14.035(3)
c (Å)	15.150(3)
α (°)	106.26(3)
β (°)	100.97(3)
γ (°)	104.81(3)
V (Å^3)	1420.0(5)
Z	1
D_{Calcd} (g cm^{-3})	1.959
μ (mm^{-1})	3.369
F (0 0 0)	830
Reflections collected/unique	13,641/5,130
R(int)	0.0387
GOF on F^2	1.010
R_1[a], wR_2 [$I > 2\delta(I)$]	0.0715, 0.1951
R_1, wR_2 (all data)	0.0897, 0.2099
ρ_{fin} (max/min) (e Å^{-3})	0.977, −2.787

[a] $R_1 = \sum(|F_o| - |F_c|)/\sum|F_o|$, $wR_2 = [\sum w(F_o^2 - F_c^2)^2/\sum w(F_o^2)^2]^{0.5}$.

Table 2. Selected bond lengths [Å] and angles [°] for **1**.

Cu(1)–X3	1.851(7)	X3-Cu(1)-N(7)	147.4(3)
Cu(1)–N(7)	1.929(6)	X3–Cu(1)–N(11)#1	102.2(3)
Cu(1)–N(11)#1	2.132(6)	N(7)–Cu(1)–N(11)#1	110.3(2)
Cu(2)–X4	1.874(8)	X4–Cu(2)–X1	151.3(3)
Cu(2)–X1	1.893(7)	X4–Cu(2)–N(8)	106.1(3)
Cu(2)–N(8)	2.133(6)	X1–Cu(2)–N(8)	102.6(3)
Cu(3)–N(9)	1.890(6)	N(9)#2–Cu(3)–N(9)	180.0(2)
Cu(4)–X2	1.870(9)	X2–Cu(4)–X7	142.0(4)
Cu(4)–X7	1.902(8)	X2–Cu(4)–N(10)	117.6(3)
Cu(4)–N(10)	2.097(7)	X7–Cu(4)–N(10)	100.4(3)
Cu(5)–X5	1.887(8)	X5–Cu(5)–X6	147.5(3)
Cu(5)–X6	1.898(8)	X5–Cu(5)–N(5)#3	111.1(3)
Cu(5)–N(5)#3	2.127(7)	X6–Cu(5)–N(5)#3	101.1(3)

The disorder C/N positions in cyanide groups are treated by adopting 50% C and N occupancies at those sites and labeled as *X*. Symmetry transformations used to generate equivalent atoms: #1: $x, y, z-1$; #2: $-x-1, -y+2, -z-2$; #3: $x, y-1, z$.

3. Results and discussion

3.1. *Description of crystal structure*

X-ray single-crystal diffraction analysis showed that **1** crystallized in the triclinic space group $P-1$, and the asymmetric unit consists of five Cu^+ ions, one NH_2-BPT ligand, one BPT ligand, and three and a half cyanide anions. NH_2-BPT deaminized to form the new ligand BPT under the hydrothermal synthesis conditions, which was essential to bind the metal ions in a multidentate fashion and to provide a negative charge to balance the overall charge of the porous framework. A similar deaminization of the triazolate ligand has been observed in our previous work [28]. NH_2-BPT and BPT take the *transoid*- and *cisoid*-configurations, respectively. The central triazole ring and two 3-pyridyl groups in *transoid*-NH_2-BPT are basically co-planar, however, the dihedral angles between the triazole ring and two 3-pyridyl groups in *cisoid*-BPT are about 30°. These are comparable to those found in other structurally characterized complexes with pyridyl-substituted 1,2,4-triazole ligands, such as the 1-D Cu(I)-3,5-di-2-pyridyl-1,2,4-triazolate meso-helical chain reported by Cheng and co-authors [29].

As shown in figure 1, four of the five independent copper centers (Cu1, Cu2, Cu4, and Cu5) have distorted trigonal coordination geometries. However, the detailed coordination environments are different. Cu_1 is coordinated by one pyridyl N atom from NH_2-BPT, one triazole N atom from BPT, and one μ_2-bridging cyanide group. Cu_2 and Cu_5 are coordinated by one pyridyl N atom from BPT and two μ_2-bridging cyanide groups. One pyridyl N atom from NH_2-BPT and two μ_2-bridging cyanide groups surround Cu_4. The remaining Cu_3 atom has a linear coordination geometry generated by two triazole N atoms from two different BPT ligands. The $Cu–N_{(triazole)}$ and Cu–X (X represents the disordered C/N positions in the cyanide groups, treated by adopting 50% C and N occupancies in each position) bond lengths are 1.890(6)–1.929(6) and 1.851(7)–1.902(8) Å, respectively, while the $Cu–N_{(pyridyl)}$ bond lengths are 2.097(7)–2.133(6). All these distances are comparable with those observed in other reported Cu(I) or cyanide coordination compounds, such as $[(phpzm)Cu(\mu\text{-}CN)]_n$ (phpzm = bis(4-phenyl-pyrazol-1-yl)methane) [30], $[Cu^{II}Cu^{I}(\mu_{1,3}\text{-}SCN)_2(\mu_{1,1,3}\text{-}SCN)(PhenE)]_n$ (PhenE = 2-ethoxy-1,10-phenanthroline) [31], and $[Cu_2(\mu\text{-}I)_2(\mu\text{-}(4\text{-}NO_2Ph)_2dapte)]_n$ ($(4\text{-}NO_2Ph)_2$dapte = *N*,*N′*-di-(4-nitrobenzaldimine)-1,2-di(o-aminophenylthio)

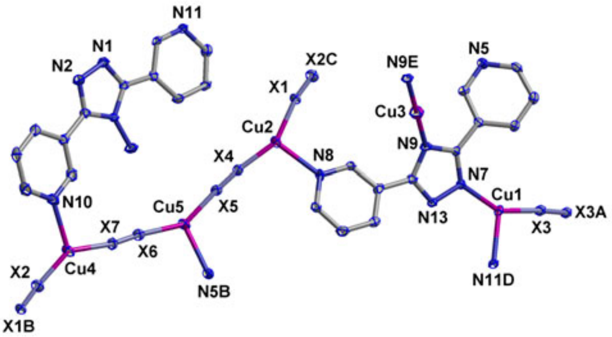

Figure 1. View of the basic coordination environment for **1**, with *xx*% probability ellipsoids. The disorder C/N positions in cyanide groups are treated by adopting 50% C and N occupancies at those sites and labeled as *X* (*X*1 = 0.5 N6 + 0.5 C27′, *X*2 = 0.5 N6′ + 0.5 C27, *X*3 = 0.5 N12 + 0.5 C28, *X*4 = 0.5 N14 + 0.5 C21′, *X*5 = 0.5 N14′ + 0.5 C21, *X*6 = 0.5 N15 + 0.5 C10′, *X*7 = 0.5 N15′ + 0.5 C10). [Symmetry codes: (A) $A-2-x,\ 2-y,\ -3-z$; (B) $x,\ -1+y,\ z$; (C) $x,\ 1+y,\ z$; (D) $x,\ y,\ -1+z$; (E) $-1-x,\ 2-y,\ -2-z$]. [au: I do not know the % probability ellipsoids nor the significance of the apostrophes after the atom labels. Neither do I see the relevance of the symmetry codes.]

ethane) [32]. The X–Cu–N and X–Cu–X bond angles are 100.4(3)–147.4(3)° and 142.0(4)–151.3(3)°, respectively. As depicted in figure 2(a), Cu_2, Cu_4, Cu_5, one *cisoid*-BPT, and two CN^- anions link together to form a $[Cu_3C_8N_5]$ sixteen-membered organic–inorganic hybrid ring. Two such ringed motifs are joined together by a Cu_3 atom through the N(4)-position (atom N(9)) of the triazole ring generated by *in situ* deaminization to give a $[Cu_7(BPT)_2(CN)_4]$ hybrid heptanuclear cluster with Cu_3 at the inversion center. There are $\pi\cdots\pi$ stacking interactions between the 3-pyridyl rings of this cluster, with a centroid-to-centroid distance of 3.977(6) Å and a dihedral angle between the pyridyl rings of 10.53°, which may help to stabilize this hybrid cluster. To the best of our knowledge, such a hybrid heptanuclear cluster is unprecedented.

Each $[Cu_7(BPT)_2(CN)_4]$ cluster connects two adjacent heptanuclear clusters along the *b*-axis through a double bridging mode via four CN^- anions (figure 2(b)). Furthermore, four $[Cu_1–CN–Cu_1]$ binuclear clusters are also linked through two triazole N(1)-positions (atom N(7)) and two *transoid*-NH_2-BPT ligands. As well, each $[Cu_1–CN–Cu_1]$ binuclear unit connects four adjacent $[Cu_7(BPT)_2(CN)_4]$ hybrid clusters as shown in figure 2(c). Thus, two kinds of subunits are interlinked to generate a complicated 3-D hybrid framework. From a topological viewpoint, these two building blocks can be defined as 4- and 6-connected nodes (figure 2(d) and (e)), and NH_2-BPT as a linker. Thus, the whole hybrid framework of **1** can be simplified to a (4,6)-connected topological net (figure 2(f)) with node–node distances of 7.8, 14.1, and 15.7 Å. The Schläfli symbol for the net is $(4^4\times6^2)(4^4\times6^{10}\times8)$, representing the 4-connected $[Cu_1–CN–Cu_1]$ node and the 6-connected $[Cu_7(BPT)_2(CN)_4]$ node, respectively.

Additionally, the 3-D hybrid framework of **1** also exhibits a layer–layer packing motif. As shown in figure 3(a), the $[Cu_3C_8N_5]$ 16-membered hybrid rings mentioned above are connected by CN^- anions to form a 1-D chain, and then are linked by Cu_1 and NH_2-BPT to form a 2-D hybrid single-layer structure in the *bc*-plane. Further, two single layers are joined together through another CN^- anion to generate a double-layer structure, with the two single layers symmetrically distributed. This neutral, double-layered coordination polymer has been reported by Guo and co-authors [24]. The deamination of NH_2-BPT did not occur in their work. In our opinion, although the hydrothermal conditions are similar, the increased CuCN

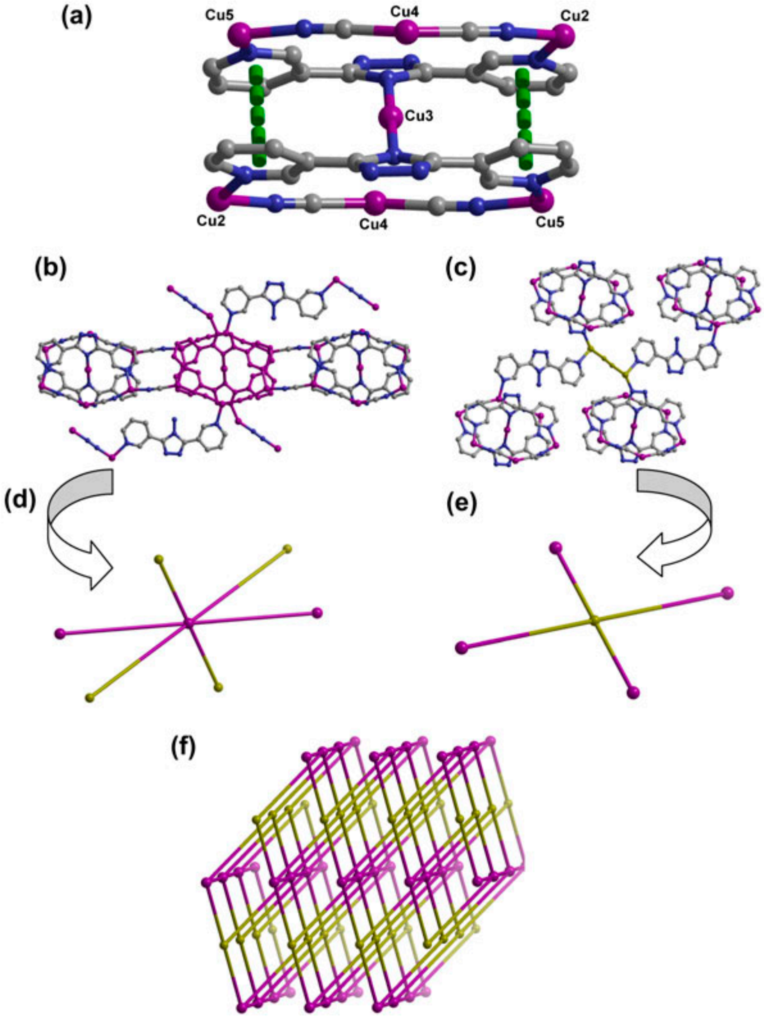

Figure 2. (a) The [$Cu_7(BPT)_2(CN)_4$] heptanuclear hybrid cluster. (b) The linkage around each heptanuclear motif. (c) The linkage around each [Cu_1–CN–Cu_1] binuclear cluster. (d) The topological representation of the 6-connected node. (e) The topological representation of the 4-connected node. (f) The (4,6)-connected 3-D topological framework of **1**.

to ligand molar ratio and the longer reaction time in our experiments led to *in situ* deamination of NH_2-BPT. The *in situ* generated unoccupied N(9) atom of the BPT triazole ring is coordinated to Cu_3, and ultimately extends the double layers to form a 3-D hybrid framework exhibiting … A-CN-B-Cu_3-A-CN-B-Cu_3 … layer–layer packing (figure 3(b)).

3.2. *XRPD, FT-IR, Raman spectrum, and TGA*

Compound **1** was also characterized by PXRD at room temperature (figure 4(a)). The PXRD pattern measured for the as-synthesized sample was in agreement with the PXRD pattern

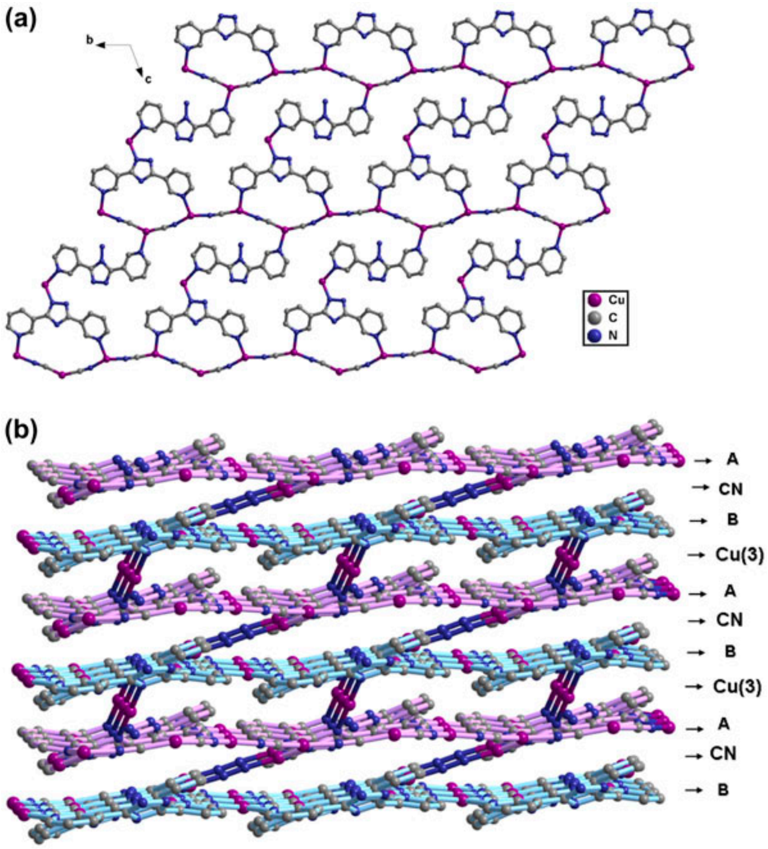

Figure 3. (a) The hybrid single-layer structure in the *bc*-plane. (b) The layer–layer packing framework of **1**.

simulated from the single-crystal X-ray data, which indicates the high purity of bulk sample. The FT-IR spectrum (figure 4(b)) exhibited a strong single band at 2125 cm^{-1}, which is typical for a bridging cyanide group and consistent with that observed in Fe [33, 34] and Ni [35, 36] cyanide compounds. This result is consistent with the single-crystal structure of **1**, which shows four μ_2-bridging cyanide groups. The other two series of bands in the ranges of 421–1598 and 2851–3344 cm^{-1} are ascribed to the vibrations of NH_2-BPT and BPT ligands. The medium strong intensity band at 3344 cm^{-1} can be assigned to the vibration of $-NH_2$ group. The bands at 3062 and 2923 cm^{-1} are consistent with the characteristic *v*(CH) stretching frequency of the pyridine rings. The framework vibrations of the pyridine and triazole rings are observed from 1325 to 1598 cm^{-1}. Similarly, the Raman spectrum exhibited a strong band at 2130 cm^{-1} associated with bridging CN^- anions. The band at 3071 cm^{-1} can be assigned to the *v*(CH) stretching vibrations. A series of bands at 1601, 1508, 1451, and 1421 cm^{-1} can be assigned to the stretching vibrations of triazole and pyridine aromatic rings. The C-C framework vibrations of pyridine are observed at 1021 cm^{-1}. Compound **1** was characterized by thermal analysis under nitrogen gas from 40 to 1000 °C (figure 4(c)). The TG curve supports the chemical composition of **1**. The data show that **1** was stable to

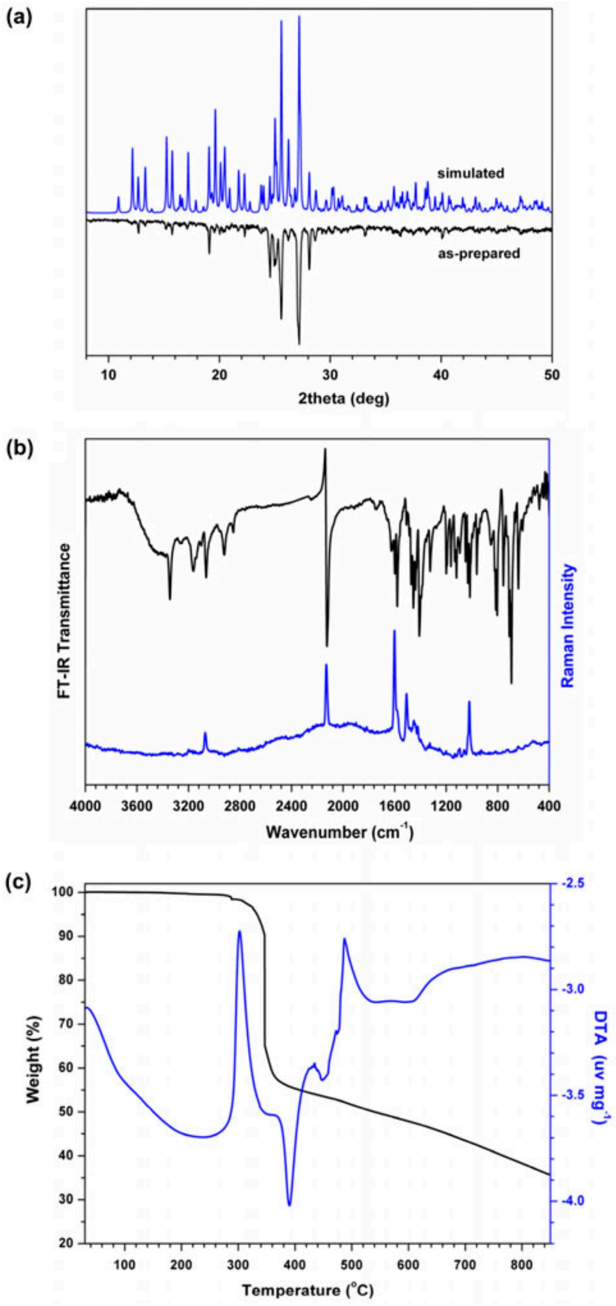

Figure 4. (a) The experimental and simulated X-ray powder diffraction patterns for **1**. (b) FT-IR and Raman spectra for **1**. (c) TG/DTA curves of **1**.

ca. 300 °C. From 300 to 400 °C, there was a sharp weight loss was due to the decomposition of NH_2-BPT and BPT (exptl: 46.2%, Calcd: 45.0%). Subsequently, the *in situ* generated

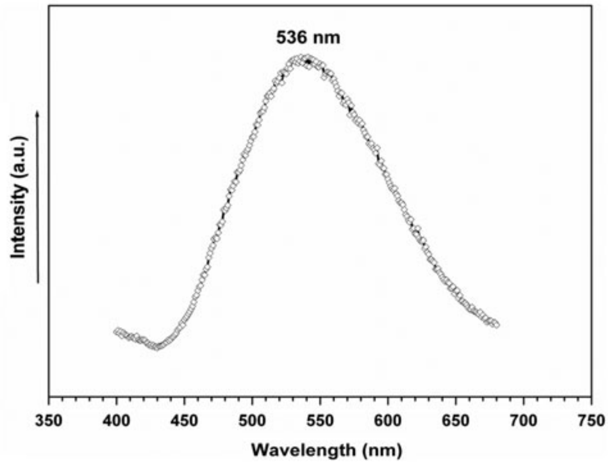

Figure 5. Solid-state emission spectrum of **1** at ambient temperature.

CuCN solid slowly decomposed with increasing temperature, and the final residue corresponds to copper powder (exptl: 35.4%, Calcd: 34.1%).

3.3. *Solid-state photoluminescence property*

Many reports have shown that the emission energies of Cu(I) halide or pseudohalide complexes are strongly affected by the organic spacers, and several possible lowest excited states such as CC, LC, XLCT, and MLCT have been proposed [37–39]. On the other hand, the luminescent properties of metal 1,2,4-triazolate polynuclear compounds or coordination polymers explored by us and others have also indicated that emission spectra of organic ligands were remarkably affected by their incorporation into metal-containing coordination compounds [40–43]. Thus, we speculate that the Cu(I)–CN–triazolate framework of **1** should exhibit interesting photoluminescence properties. As shown in figure 5, upon excitation of the solid samples at λ = 344 nm, intense bands in the emission spectra are observed at 536 nm for **1**. The lowest unoccupied molecular orbitals in **1** are mainly associated with the Cu–N δ^*-antibonding orbitals, localized more on the metal centers, whereas the highest occupied molecular orbitals are presumably associated with the π-bonding orbitals from the aromatic triazole or pyridine rings, or CN^- anions. Consistent with the previously reported complexes of cuprous pseudohalides and N-heterocyclic ligands, we have tentatively assigned the emission of **1** as a MLCT transition (Cu → triazole, Cu → pyridine, or Cu → CN) due to the broad and structureless emission spectrum [37–39].

4. Conclusion

Both cuprous cyanide systems and polyazaheteroaromatic ligands have attracted interest for constructing metal-organic coordination compounds. Utilizing self-assembly of an angular dipyridine derivative of 1,2,4-triazole with CuCN, we isolated a (4,6)-connected Cu(I)–CN–triazolate framework based on a unique heptanuclear hybrid cluster. The structural analysis shows that *in situ* deaminization of NH_2-BPT is an essential factor for generation of this 3-D layer–layer packed structure. Further investigations of new hybrid solids based on five-membered N-heterocyclic ligands and Cu(I) halides or pseudohalides are ongoing in our lab.

Funding

This work was supported by the National Natural Science Foundation of China [21271123]; New Century Excellent Talents in University [NCET-12-0897]; and the Fundamental Research Funds for the Central Universities [GK201102004].

References

[1] Y. Chujo. *Curr. Opin. Solid State Mater. Sci.*, **1**, 806 (1996).
[2] S.R. Batten, R. Robson. *Angew. Chem. Int. Ed.*, **37**, 1460 (1998).
[3] O.R. Evans, W. Lin. *Acc. Chem. Res.*, **35**, 511 (2002).
[4] S.R. Batten, K.S. Murray. *Coord. Chem. Rev.*, **246**, 103 (2003).
[5] S. Kitagawa, R. Kitaura, S. Noro. *Angew. Chem. Int. Ed.*, **43**, 2334 (2004).
[6] X.M. Chen, M.L. Tong. *Acc. Chem. Res.*, **40**, 162 (2007).
[7] N.W. Ockwig, O. Delgado-Friedrichs, M. O'Keeffe, O.M. Yaghi. *Acc. Chem. Res.*, **38**, 176 (2005).
[8] D.J. Chesnut, J. Zubieta. *Chem. Commun.*, **34**, 1707 (1998).
[9] F.B. Stocker, T.P. Staeva, C.M. Rienstra, D. Britton. *Inorg. Chem.*, **38**, 984 (1999).
[10] Z. Li, M. Li, S.Z. Zhan, X.C. Huang, S.W. Ng, D. Li. *CrystEngComm.*, **10**, 978 (2008).
[11] F. Wang, J. Zhang, S.M. Chen, Y.M. Xie, X.Y. Wu, S.C. Chen, R.M. Yu, C.Z. Lu. *CrystEngComm.*, **11**, 1562 (2009).
[12] D.J. Chesnut, A. Kusnetzow, R. Birge, J. Zubieta. *Inorg. Chem.*, **38**, 5484 (1999).
[13] A.X. Zhu, Q.Q. Xu, F.Y. Liu, X.L. Qi. *Z. Anorg. Allg. Chem.*, **637**, 502 (2011).
[14] X. He, C.Z. Lu, C.D. Wu, L.J. Chen. *Eur. J. Inorg. Chem.*, **2006**, 2491 (2006).
[15] X.M. Zhang, Y.F. Zhao, W.X. Zhang, X.M. Chen. *Adv. Mater.*, **19**, 2843 (2007).
[16] Y.B. Dong, H.Y. Wang, J.P. Ma, R.Q. Huang. *Cryst. Growth Des.*, **5**, 789 (2005).
[17] M. Du, Z.H. Zhang, X.J. Zhao, Q. Xu. *Inorg. Chem.*, **45**, 5785 (2006).
[18] Y.B. Dong, T. Sun, J.P. Ma, X.X. Zhao, R.Q. Huang. *Inorg. Chem.*, **45**, 10613 (2006).
[19] M. Du, Z.H. Zhang, L.F. Tang, X.G. Wang, X.J. Zhao, S.R. Batten. *Chem.-Eur. J.*, **13**, 2578 (2007).
[20] M. Du, Z.H. Zhang, Y.P. You, X.J. Zhao. *CrystEngComm.*, **10**, 306 (2008).
[21] Q.G. Zhai, J.P. Niu, M.C. Hu, Y. Wang, W.J. Ji, S.N. Li, Y.C. Jiang. *J. Coord. Chem.*, **62**, 2927 (2009).
[22] Q.G. Zhai, M.C. Hu, Y. Wang, W.J. Ji, S.N. Li, Y.C. Jiang. *Inorg. Chem. Commun.*, **12**, 286 (2009).
[23] Q.G. Zhai, R. Ding, S.N. Li, W.J. Ji, X. Gao, Y.C. Jiang, M.C. Hu. *Inorg. Chim. Acta*, **363**, 653 (2010).
[24] H.M. Guo, X. He, J.J. Liu, J. Han, M.X. Li. *Polyhedron*, **30**, 1982 (2011).
[25] R.M. Herbst, J.A. Garrison. *J. Org. Chem.*, **18**, 872 (1953).
[26] G.M. Sheldrick. *SADABS, Program for Area Detector Adsorption Correction*, Institute for Inorganic Chemistry, University of Göttingen, Germany (1996).
[27] G.M. Sheldrick. *SHELXL-97, Program for Solution of Crystal Structures*, University of Göttingen, Germany (1997).
[28] Z.G. Zhao, J. Zhang, X.Y. Wu, Q.G. Zhai, L.J. Chen, S.M. Chen, Y.M. Xie, C.Z. Lu. *CrystEngComm.*, **10**, 273 (2008).
[29] L. Cheng, Q. Cao, L. Zhang, S. Gou. *J. Coord. Chem.*, **65**, 1821 (2012).
[30] H.Y. Li, Z.L. Xu, H.X. Li, Y. Zhang, L.X. Dai, J.P. Lang. *J. Coord. Chem.*, **65**, 4203 (2012).
[31] R.Z. Wei, J.M. Shi, W. Wei, S.L. Liu. *J. Coord. Chem.*, **66**, 1916 (2012).
[32] M. Rasouli, M. Morshedi, M. Amirnasr, A.M.Z. Slawin, R. Randall. *J. Coord. Chem.*, **66**, 1974 (2012).
[33] K.R. Ranjan, A. Singh, A. Banerjee, B. Singh. *J. Coord. Chem.*, **64**, 805 (2011).
[34] D. Zhang, Z. Zhao, P. Wang, X. Chen. *J. Coord. Chem.*, **65**, 2549 (2012).
[35] A. Panja. *J. Coord. Chem.*, **64**, 987 (2011).
[36] Y.M. Gayfulin, A.I. Smolentsev, Y.V. Mironov. *J. Coord. Chem.*, **64**, 3832 (2011).
[37] A. Barbieri, G. Accorsi, N. Armaroli. *Chem. Commun.*, **44**, 2185 (2008).
[38] P.C. Ford, E. Cariati, J. Bourasssa. *Chem. Rev.*, **99**, 3625 (1999).
[39] C. Kutal. *Coord. Chem. Rev.*, **99**, 213 (1990).
[40] J.P. Zhang, Y.Y. Lin, X.C. Huang, X.M. Chen. *J. Am. Chem. Soc.*, **127**, 5495 (2005).

[41] Y.B. Dong, J.Y. Cheng, H.Y. Wang, R.Q. Huang, B. Tang, M.D. Smith, H.C. zur Loye. *Chem. Mater.*, **15**, 2593 (2003).
[42] Y.B. Dong, J.Y. Cheng, R.Q. Huang, B. Tang, M.D. Smith, H.C. zur Loye. *Inorg. Chem.*, **42**, 5699 (2003).
[43] Q.G. Zhai, M.C. Hu, S.N. Li, Y.C. Jiang. *Inorg. Chem. Commun.*, **11**, 1147 (2008).